A Comparison between Star and Delta Connected Induction Motors when Supplied by Current Source Inverters

P. PILLAY, R. G. HARLEY and E. J. ODENDAL

Department of Electrical Engineering, University of Natal, King George V Avenue, Durban 4001 (South Africa)

(Received April 9, 1984)

SUMMARY

This paper analyses whether any differences in behaviour arise due to an induction motor being star or delta connected when supplied by a current source inverter. Two comparisons are considered. The first is that of a delta connected motor compared to a star connected motor of the same power and voltage ratings; the star connected motor in this case is then mathematically the delta connected motor's equivalent star connection. The second case considered is that of a delta connected motor rewired as a star connected motor.

1. INTRODUCTION

The induction motor is robust and cheap and with the advent of power semiconductors is being used widely in variable speed applications. Frequency conversion usually takes place by first rectifying the fixed AC mains and then inverting to a new variable frequency. The DC link between rectifier and inverter can be operated with the link voltage held constant, or with the link current held constant; the latter method is illustrated in Fig. 1 and is usually referred to as a current source inverter (CSI).

Sinusoidal currents cannot be applied to the motor from a CSI inverter; instead quasi-square blocks [1] of current are applied which adversely affect the motor operation [1 - 3]. Some investigations [2, 3] have considered star connected induction motor stators while others [4, 5] have evaluated delta connections. A comparison of the behaviour due to either a star or delta connected stator has not been presented.

The purpose of this paper is therefore to investigate whether any differences in behavior arise due to the method of stator connection of a CSI-fed motor with special reference to the torque harmonics. The paper firstly evaluates the behaviour of the motor with phases A, B and C connected in delta, and uses the current waveforms as shown in Fig. 2. It then evaluates the performance of this

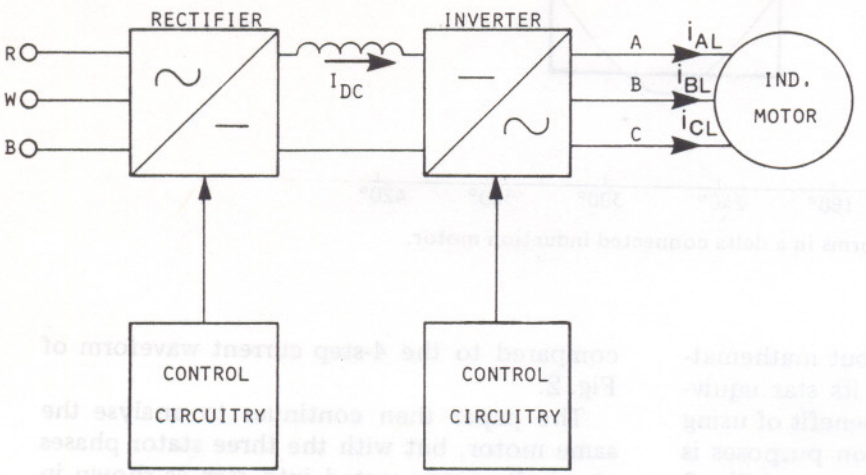

Fig. 1. Current source inverter-fed induction motor drive.

0378-7796/84/$3.00

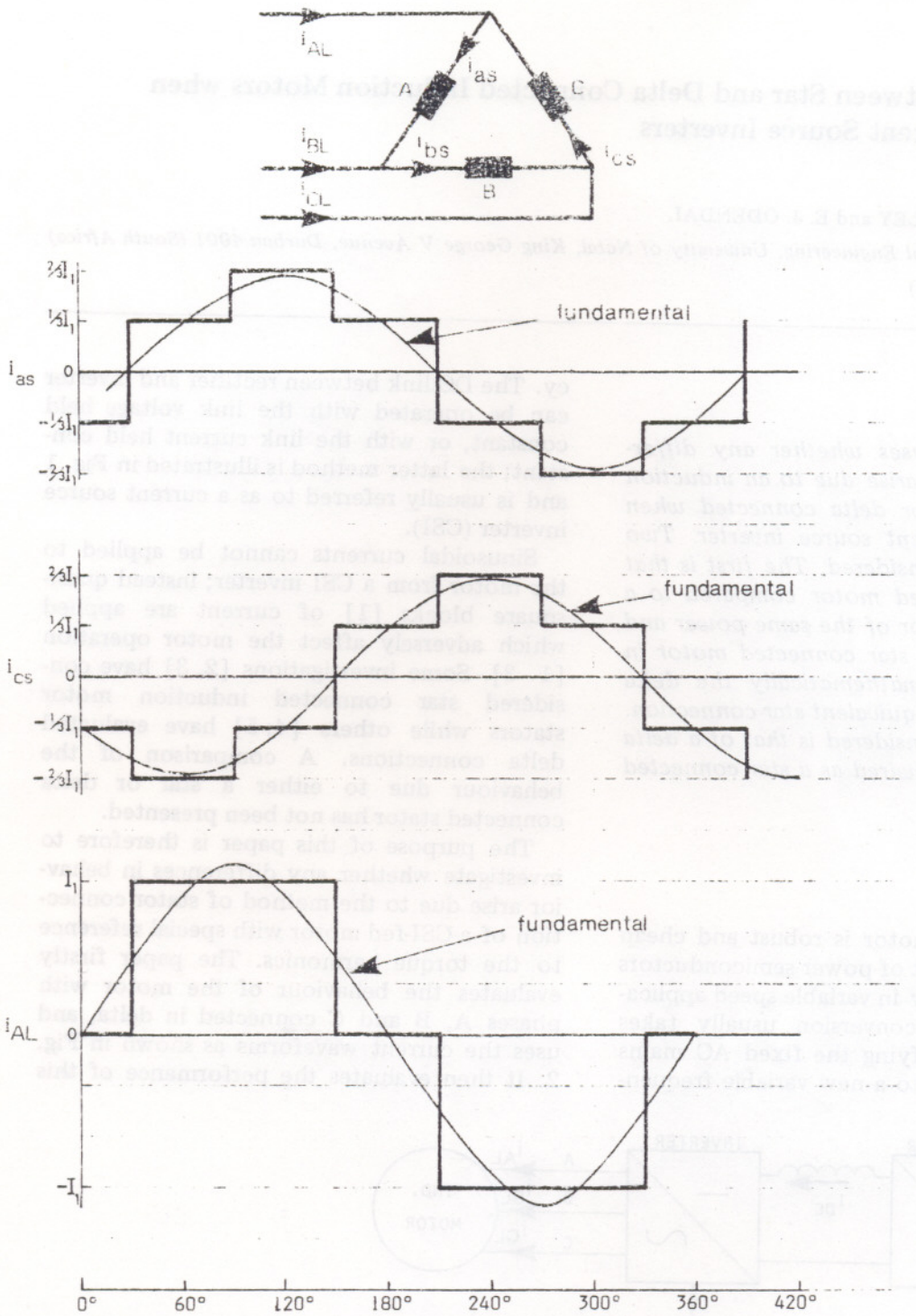

Fig. 2. Line and phase current waveforms in a delta connected induction motor.

same delta connected motor, but mathematically represents the delta by its star equivalent as shown in Fig. 3. The benefit of using an equivalent star for simulation purposes is the simpler 3-step current waveform of Fig. 3 compared to the 4-step current waveform of Fig. 2.

The paper then continues to analyse the same motor, but with the three stator phases physically reconnected into star as shown in

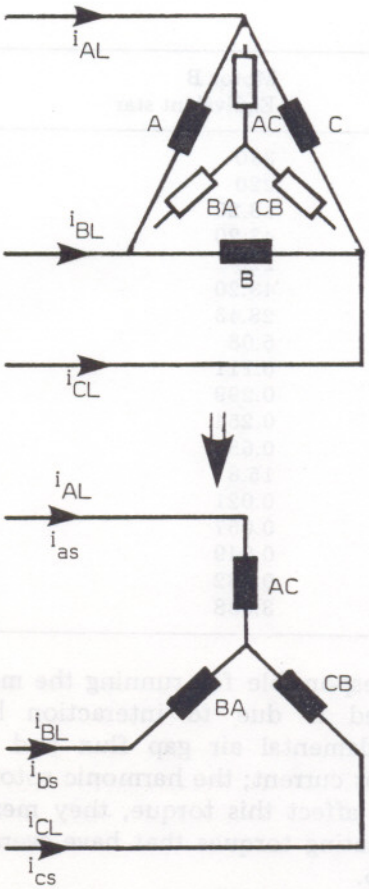

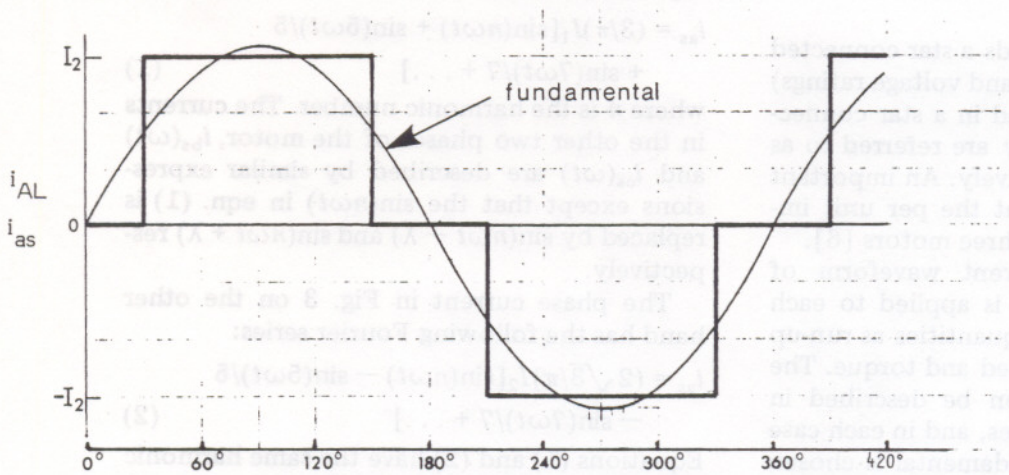

Fig. 3. Line and phase current waveforms in a star connected induction motor.

Fig. 4 in order to establish whether the actual connection has any effect on the motor performance.

In these comparisons particular attention is paid to torque harmonics.

2. THEORY

2.1. Analysis of the current waveforms

Table 1 shows a list of motor parameters in terms of the original delta winding, the equiv-

TABLE 1

Motor parameters

	Motor A Delta	Motor B Equivalent star	Motor C Star
Line voltage (V)	380	380	658
Phase voltage (V)	380	220	380
Line current (A)	43.20	43.20	24.94
Phase current (A)	24.94	43.20	24.94
Base voltage (phase) (V)	380	220	380
Base current (phase) (A)	24.94	43.20	24.94
Base power ($3V_{ph}I_{ph}$) (kVA)	28.43	28.43	28.43
Base impedance (V_{ph}/I_{ph}) (Ω)	15.24	5.08	15.24
Stator resistance (Ω)	0.333	0.111	0.333
Rotor resistance (Ω)	0.897	0.299	0.897
Stator leakage reactance (Ω)	0.762	0.254	0.762
Rotor leakage reactance (Ω)	2.052	0.684	2.052
Magnetizing reactance (Ω)	47.4	15.8	47.4
Stator resistance (p.u.)	0.021	0.021	0.021
Rotor resistance (p.u.)	0.057	0.057	0.057
Stator leakage reactance (p.u.)	0.049	0.049	0.049
Rotor leakage reactance (p.u.)	0.132	0.132	0.132
Magnetizing reactance (p.u.)	3.038	3.038	3.038

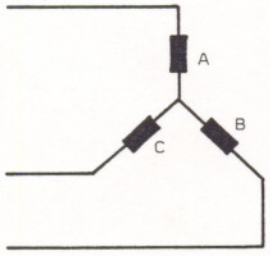

Fig. 4. Delta winding reconnected in star.

alent star (or in other words a star connected motor of the same power and voltage ratings) and the motor reconnected in a star connection; for convenience they are referred to as motors A, B and C respectively. An important result from Table 1 is that the per unit impedances are equal for all three motors [6].

The characteristic current waveform of each winding (Figs. 2 - 4) is applied to each motor to determine such quantities as run-up time, terminal voltage, speed and torque. The currents in Figs. 2 - 4 can be described in terms of their Fourier series, and in each case the peak value of the fundamental is chosen as 1 p.u. This ensures that all three motors are able to supply the same output power. Also it is known [5, 7] that the magnitude of the fundamental component of current determines the average response of the induction motor (for example run-up time), with the harmonic currents having only parasitic effects. For example, the average torque that is responsible for running the machine up to speed is due to interaction between the fundamental air gap flux and fundamental rotor current; the harmonic rotor currents do not affect this torque, they merely produce pulsating torques that have average values of zero.

The phase current in Fig. 2 has the following Fourier series:

$$i_{as} = (3/\pi)I_1[\sin(n\omega t) + \sin(5\omega t)/5 + \sin(7\omega t)/7 + \ldots] \quad (1)$$

where n is the harmonic number. The currents in the other two phases of the motor, $i_{bs}(\omega t)$ and $i_{cs}(\omega t)$ are described by similar expressions except that the $\sin(n\omega t)$ in eqn. (1) is replaced by $\sin(n\omega t - \lambda)$ and $\sin(n\omega t + \lambda)$ respectively.

The phase current in Fig. 3 on the other hand has the following Fourier series:

$$i_{as} = (2\sqrt{3}/\pi)I_2[\sin(n\omega t) - \sin(5\omega t)/5 - \sin(7\omega t)/7 + \ldots] \quad (2)$$

Equations (1) and (2) have the same harmonic components except for 180° phase shifts in the 5th, 7th, 17th, 19th, etc. harmonics. The fundamental components of the two phase currents are drawn in Figs. 2 - 4; in the delta case the magnitude of the fundamental component is $(3/\pi)I_1 = 0.955\ I_1$, whereas in the star case the magnitude of the fundamental component is $(2\sqrt{3}/\pi)I_2 = 1.103\ I_2$; that is,

the fundamental component of current is smaller than the peak value of the delta waveform but larger than the peak value of the star waveform. Hence to ensure a 1 p.u. fundamental component in the delta case (motor A), I_1 is chosen equal to 1.047 p.u., while to ensure a 1 p.u. fundamental component in the star cases (B and C), I_2 is chosen equal to 0.91 p.u.

Since all the harmonics have amplitudes that are inversely proportional to their order, the amplitudes of the corresponding harmonics of the delta and star waveforms are equal if their fundamental components are equal.

2.2. Two-axis analysis of the CSI-fed induction motor

The analysis of the CSI-fed induction motor, summarized below, is based on the well-known [8] two-axis theory. An idealized symmetric motor is assumed with a balanced sinusoidal airgap mmf and a linear magnetic circuit. Iron and mechanical losses, stray load losses and mechanical damping are all neglected. All motor resistances and inductances are independent of frequency, which limits the usefulness of these models to wound rotor and single cage rotors with shallow bars.

The two-axis voltage equations of a voltage-fed induction motor can be summarized as follows in terms of a reference frame rotating in synchronism with the fundamental component of the stator current:

$$[v] = [R][i] + [L]p[i] + \omega_i[F][i] + s\omega_i[G][i] \tag{3}$$

where

$$[v] = [v_{d1}, v_{q1}, v_{d2}, v_{q2}]^T \tag{4}$$

$$[i] = [i_{d1}, i_{q1}, i_{d2}, i_{q2}]^T \tag{5}$$

$$s = (\omega_i - \omega_r)/\omega_i \tag{6}$$

The other matrices in eqn. (3) appear in Appendix C. Moreover, in the case of a current source inverter, i_{d1} and i_{q1} are independent predefined variables (obtained from Park's transform of i_{as}, i_{bs} and i_{cs}) and differential equations are only required for the rotor or secondary currents i_{d2} and i_{q2} such that [4]

$$[v_2] = [R_2][i_2] + [L_2]p[i_2] + [L_m]p[i_1] + \omega_i[G_1][i_1] + s\omega_i[G_2][i_2] \tag{7}$$

where

$$[v_2] = [v_{d2}, v_{q2}]^T$$
$$[i_2] = [i_{d2}, i_{q2}]^T \tag{8}$$
$$[i_1] = [i_{d1}, i_{q1}]^T$$

The other matrices in eqn. (7) appear in Appendix C. In a short-circuited rotor v_{d2} and v_{q2} are zero, in which case eqn. (8) can be rearranged to yield the following differential equations for the rotor currents in state space form:

$$p[i_2] = -[B]\{[R_2] + s\omega_i[G_2][i_2] + s\omega_i[G_1][i_1] + [L_m]p[i_1]\} \tag{9}$$

where $[B] = [L_2]^{-1}$. Equation (9) is nonlinear and is integrated numerically step by step to yield values for i_{d2} and i_{q2}, and together with i_{d1} and i_{q1} these are used to compute the electrical torque T_e from

$$T_e = L_m\omega_b(i_{d2}i_{q1} - i_{q2}i_{d1})/3 \tag{10}$$

The mechanical motion is described by

$$p\omega_r = (T_e - T_L)/J \tag{11}$$

For a sinusoidal line current to the motor i_{d1} and i_{q1} are constant quantities in a synchronously rotating reference frame. However, in the case of an inverter-fed motor, where the line current consists of a series of harmonics (eqns. (1) and (2)), i_{d1} and i_{q1} are functions of time and are defined by the Park transform operating on each harmonic component and summing the result. Expressions for pi_{d1}, pi_{q1} are required in eqn. (9) and are found by differentiating the summed series expressions for i_{d1} and i_{q1}, as shown in Appendix D.

A computer program was developed to predict the dynamic behaviour of the CSI-fed induction motor drive. The independent variables are i_{d1}, i_{q1}, pi_{d1} and pi_{q1}, and their accuracy depends on the number n of harmonics used in the Fourier series. The value of n has to be infinity in order to represent the waves in Figs. 2(b) and 3(b) exactly. However, it was shown elsewhere [4] that thirty-one ($n = 31$) current harmonics yield sufficient accuracy with the advantage of keeping computation time down.

The program starts by finding the magnitude of each of the thirty-one harmonic components. It then calculates i_{d1}, i_{q1}, pi_{d1} and pi_{q1}. From this it calculates i_{d2}, i_{q2}, T_e and ω_r as stated above at each step of the integration process.

3. RESULTS

This section uses the above techniques to evaluate the response of the delta connected motor A (which has a 4-step waveform) and of the star connected motors B and C (which have 3-step waveforms). Note that a simulation done for motor B is also true for motor C if the analysis is carried out in p.u. form, because the current waveform is the same and they have the same p.u. impedances; however, the physical magnitudes of the different variables will be different because they have different voltage and current base values. The significance of this will be explained later.

Figure 5 shows the no-load start-up results when the motor is supplied from the 10 Hz, 4-step current waveform of Fig. 2, while Fig. 6 shows the corresponding waveforms when the motor is started up from the 3-step current waveform of Figs. 3 and 4. These results show that the run-up time and torque pulsations in p.u. are exactly the same for all three motors. However, since all three machines have the same power and frequency bases, the physical magnitudes of the motor torque pulsations are also equal. The magnitude of the terminal voltages are equal, but the 3-step current waveform with four current transitions per cycle produces four voltage spikes per cycle, while the 4-step current waveform produces six voltage spikes per cycle. Since these voltage spikes stress the motor insulation, the star connected motor which produces the lower number of voltage spikes may be preferable.

Figure 7 shows the FFTs of the phase currents for the star (3-step) and delta (4-step) waveforms. The FFT of the star waveform in Fig. 7(a) shows that the fundamental component of the current is 2 p.u. peak-to-peak (the magnitude of the fundamental component of current was chosen as 1 p.u. peak); the magnitude of the fundamental component of the delta waveform in Fig. 7(b) is also 2 p.u. peak-to-peak, and the magnitudes of all the relative current harmonics in Fig. 7(b) are equal to those in Fig. 7(a). The FFTs of torque in Figs. 7(c) and (d) show that the individual torque harmonics which add up to produce the torque pulsations in Figs. 5(c) and 6(c) are also equal.

These results show that the run-up time and the magnitude of the torque pulsations are the same for the delta and star connected motors when expressed in p.u. The line current needed (this specifies the link current indirectly) is 43.2 A rms for both the delta connected motor A and the star connected motor B of the same power and voltage ratings. Hence, a given current source inverter able to supply current to motor A would also be able to supply it to motor B. The only difference in operation between these two motors is the presence of a different number of voltage spikes per cycle. However, motor C only requires 24.94 A in its line in order to supply full power. This means that the current ratings of its current source inverter can be less. Nevertheless, its terminal voltage (when it draws 24.94 A) is 658 rms, and in any practical system this voltage gets reflected back to the input voltages of the rectifier which must now be rated at 658 V rms. Hence the induction motor winding cannot be changed from delta to star when driven by a current source inverter without changing the ratings of the current source inverter itself (i.e. a reduction of its current rating by $\sqrt{3}$ and an increase of its voltage rating by $\sqrt{3}$). These results also show that, as far as the dynamics of the motor are concerned, a delta connected motor can be analysed in terms of its equivalent star connection.

4. CONCLUSIONS

This paper has compared the differences in behaviour between a delta connected motor, its star equivalent of the same power and voltage ratings and the original delta reconnected into star. Simulations have been carried out with the motors represented by their two-axis equations and their current waveforms by Fourier series. The magnitudes of the fundamental components of the phase currents for all three cases were chosen to be equal to 1 p.u. The following conclusions can be drawn:

(a) The harmonic current components present in the phase current of a delta connected induction motor fed from a CSI are the same as those present in a star connected motor.

(b) Provided the magnitudes of the fundamental components of these currents are specified as equal in p.u., the delta connected

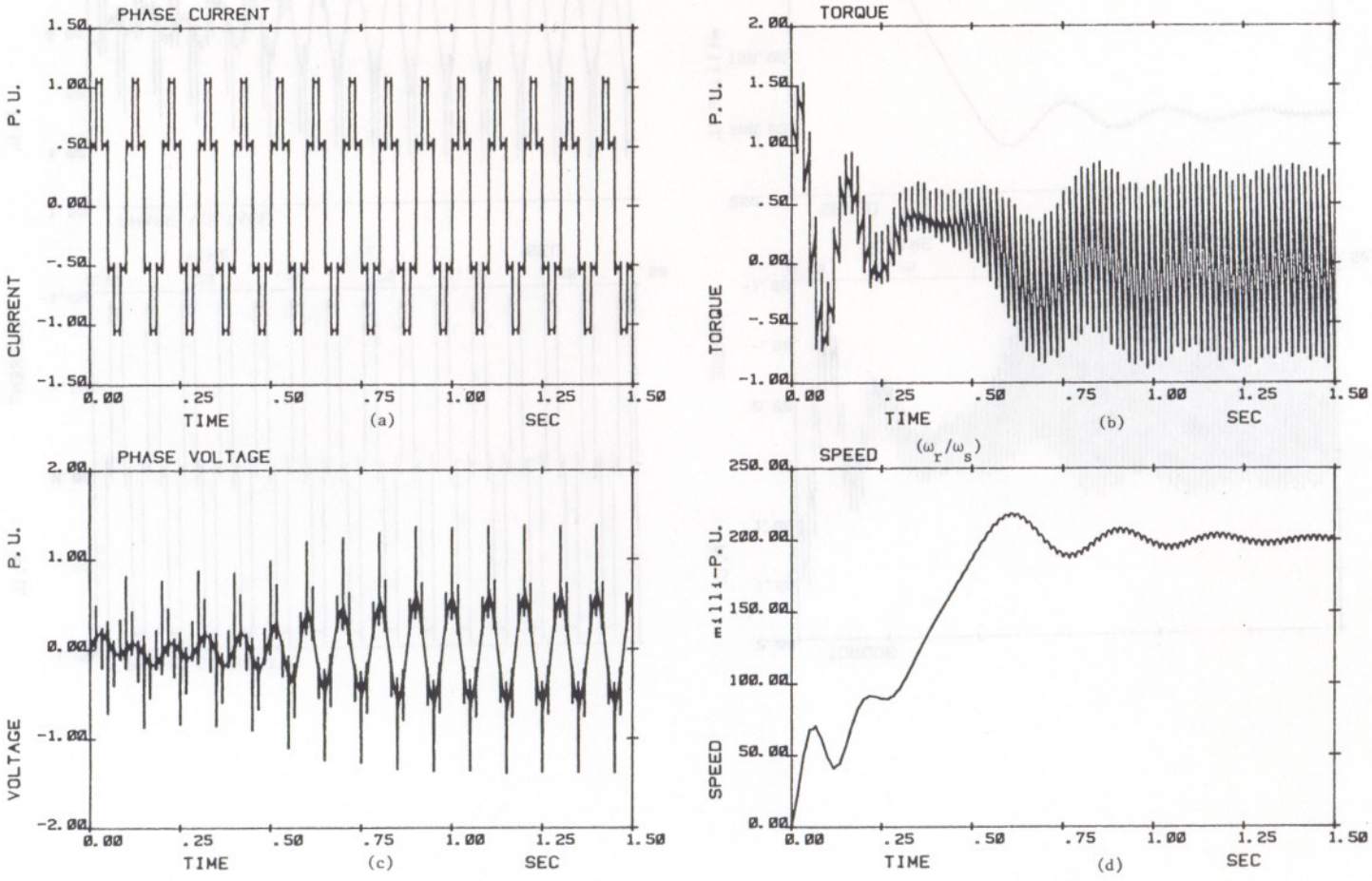

Fig. 5. Predicted start-up of a delta connected CSI-fed induction motor.

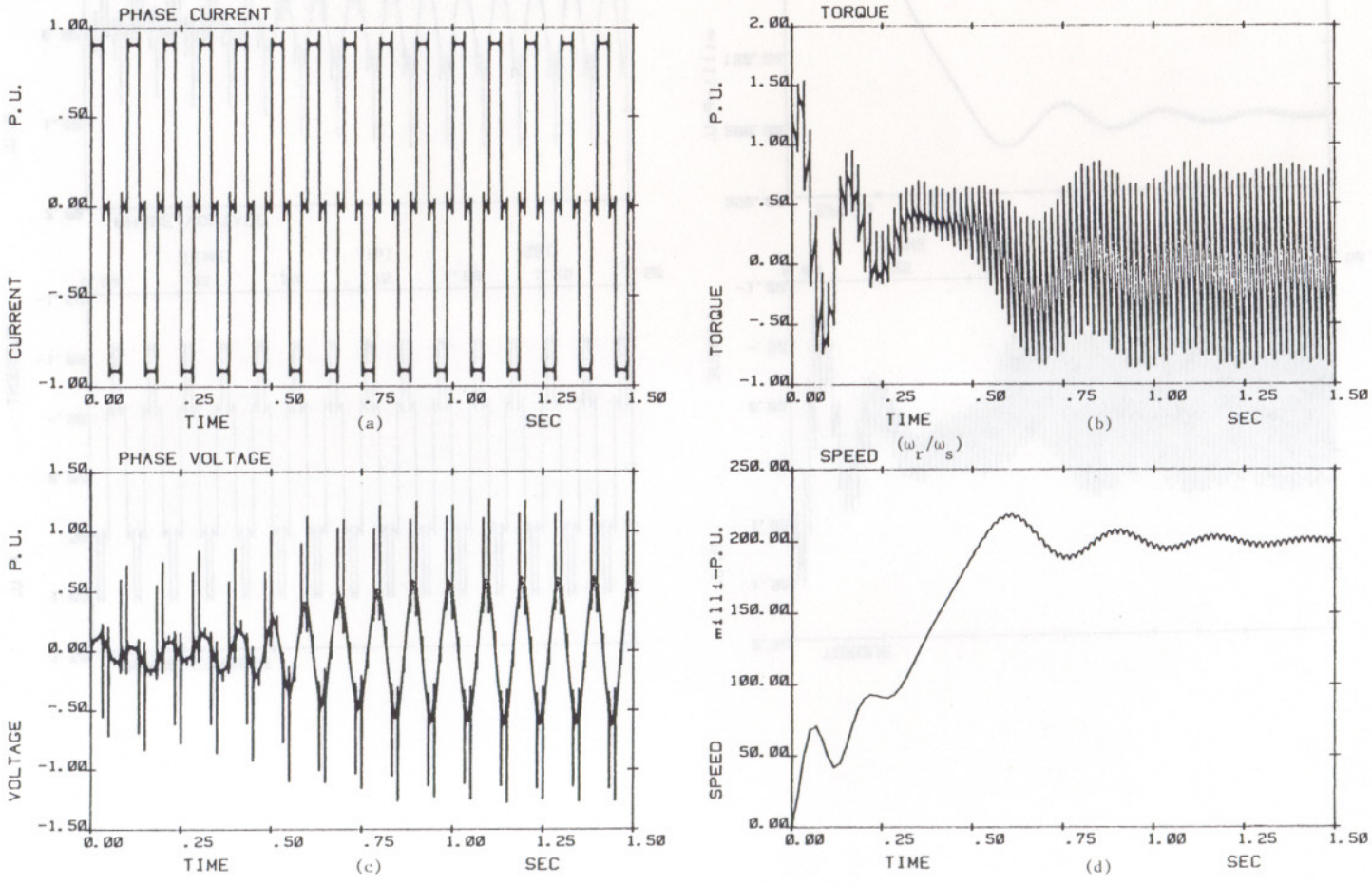

Fig. 6. Predicted start-up of a star connected CSI-fed induction motor.

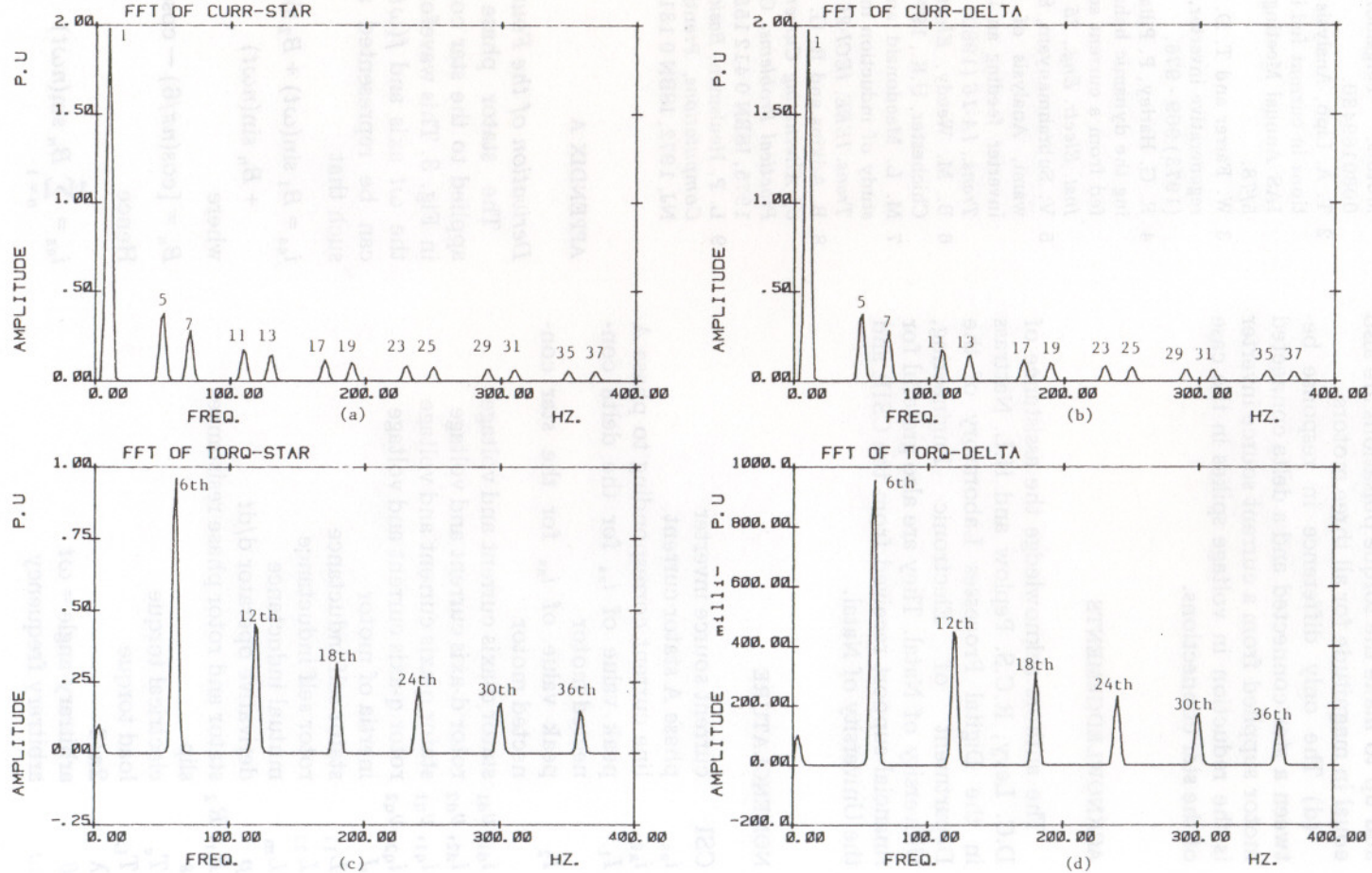

Fig. 7. FFTs of current and torque for the star and delta connected induction motors.

motor, its star equivalent and the reconnected star have the same run-up time. This also means that any delta connected motor can be analysed in terms of its star equivalent for dynamic studies.

(c) The torque pulsations produced in all three motors are the same because they all have the same power and frequency base values. Individual torque harmonics which add up to make the torque pulsations are also equal in magnitude for all three motors.

(d) The only difference in response between a star connected and a delta connected motor supplied from a current source inverter is the reduction in voltage spikes in the case of the star connections.

ACKNOWLEDGEMENTS

The authors acknowledge the assistance of D.C. Levy, R.C.S. Peplow and H.L. Nattrass in the Digital Processes Laboratory of the Department of Electronic Engineering, University of Natal. They are also grateful for financial support received from the CSIR and the University of Natal.

NOMENCLATURE

CSI	current source inverter
i_{as}	phase A stator current
$i_{a\ell}$	line current corresponding to phase A
I_1	peak value of i_{as} for the delta connected motor
I_2	peak value of i_{as} for the star connected motor
i_{d1}, v_{d1}	stator d-axis current and voltage
i_{d2}, v_{d2}	rotor d-axis current and voltage
i_{q1}, v_{q1}	stator q-axis current and voltage
i_{q2}, v_{q2}	rotor q-axis current and voltage
J	inertia of motor
L_{11}	stator self inductance
L_{22}	rotor self inductance
L_m	mutual inductance
p	derivative operator d/dt
R_1, R_2	stator and rotor phase resistances
s	slip
T_e	electrical torque
T_L	load torque
λ	$2\pi/3$
θ	arbitrary angle = ωt
ω	arbitrary frequency
ω_b	nominal frequency at which p.u. torque = p.u. power
ω_i	fundamental frequency of inverter
ω_r	rotor speed

REFERENCES

1 J. M. D. Murphy, *Thyristor Control of AC Motors*, Pergamon Press, 1973, ISBN 0080169430.

2 T. A. Lipo, Analysis and control of torque pulsations in current fed induction motor drives, IEEE IAS Annual Meeting, 1978, Paper No. CH 1337-5/78.

3 W. Farrer and T. D. Miskin, Quasi-sinewave fully regenerative inverter, *Proc. Inst. Electr. Eng., 120* (1973) 969 - 976.

4 R. G. Harley, P. Pillay and E. J. Odendal, Analysing the dynamic behaviour of an induction motor fed from a current source inverter, *Trans. S. Afr. Inst. Electr. Eng., 75* (3) (Nov./Dec.) (1984).

5 V. Subrahmanyam, S. Yuvarajan and B. Raamaswami, Analysis of commutation of a current inverter feeding an induction motor load, *IEEE Trans., IA-16* (1980) 332 - 341.

6 B. M. Weedy, *Electric Power Systems*, Wiley, Chichester, U.K., 1979, ISBN 0 471 27584 0.

7 M. L. Macdonald and P. C. Sen, Control loop study of induction motor drives using DQ model, *Trans. IEEE, IECI-26* (Nov.) (1979) 237 - 243.

8 B. Adkins and R. G. Harley, *The General Theory of Alternating Current Machines: Application to Practical Problems*, Chapman and Hall, London, 1975, ISBN 0 412 155605.

9 L. P. Heulsman, *Basic Circuit Theory with Digital Computations*, Prentice Hall, Englewood Cliffs, NJ, 1972, ISBN 0 131 57430 9.

APPENDIX A

Derivation of the Fourier series of line current

The stator phase current waveform i_{as} applied to the star connected motor is shown in Fig. 3. This waveform is symmetrical about the ωt axis and $f(\omega t) = -f(-\omega t)$. Hence i_{as} can be represented as a Fourier series [9] such that

$$i_{as} = B_1 \sin(\omega t) + B_2 \sin(2\omega t) + \ldots + B_n \sin(n\omega t) \quad \text{(A-1)}$$

where

$$B_n = [\cos(n\pi/6) - \cos(n5\pi/6)]2I_1/n\pi \quad \text{(A-2)}$$

Hence

$$i_{as} = \sum_{n=1}^{\infty} B_n \sin(n\omega t) \quad \text{(A-3)}$$

$$i_{bs} = \sum_{n=1}^{\infty} B_n \sin(n\omega t - \lambda)$$

$$i_{cs} = \sum_{n=1}^{\infty} B_n \sin(n\omega t + \lambda) \qquad \text{(A-3)}$$

This analysis is similar for the phase current waveform in Fig. 2.

APPENDIX B

Elements of matrices

$$[R] = \begin{bmatrix} R_1 & 0 & 0 & 0 \\ 0 & R_1 & 0 & 0 \\ 0 & 0 & R_2 & 0 \\ 0 & 0 & 0 & R_2 \end{bmatrix}$$

$$[L] = \begin{bmatrix} L_{11} & 0 & L_m & 0 \\ 0 & L_{11} & 0 & L_m \\ L_m & 0 & L_{22} & 0 \\ 0 & L_m & 0 & L_{22} \end{bmatrix}$$

$$[F] = \begin{bmatrix} 0 & L_{11} & 0 & L_m \\ -L_{11} & 0 & -L_m & 0 \\ 0 & 0 & 0 & 0 \\ 0 & 0 & 0 & 0 \end{bmatrix}$$

$$[G] = \begin{bmatrix} 0 & 0 & 0 & 0 \\ 0 & 0 & 0 & 0 \\ 0 & L_m & 0 & L_{22} \\ -L_m & 0 & -L_{22} & 0 \end{bmatrix}$$

$$[R_2] = \begin{bmatrix} R_2 & 0 \\ 0 & R_2 \end{bmatrix} \qquad [G_2] = \begin{bmatrix} 0 & L_{22} \\ -L_{22} & 0 \end{bmatrix}$$

$$[G_1] = \begin{bmatrix} 0 & L_m \\ -L_m & 0 \end{bmatrix} \qquad [L_m] = \begin{bmatrix} L_m & 0 \\ 0 & L_m \end{bmatrix}$$

$$[L_2] = \begin{bmatrix} L_{22} & 0 \\ 0 & L_{22} \end{bmatrix}$$

APPENDIX C

Definition of Park's orthogonal transformation matrix

$$[F_{0dq1}] = [P_\theta][F_{abc1}] \qquad \text{(C-1)}$$

where

$$[P_\theta] = \sqrt{2/3} \begin{bmatrix} \sqrt{1/2} & \sqrt{1/2} & \sqrt{1/2} \\ \cos\theta & \cos(\theta - \lambda) & \cos(\theta + \lambda) \\ \sin\theta & \sin(\theta - \lambda) & \sin(\theta + \lambda) \end{bmatrix} \qquad \text{(C-2)}$$

$$[F_{abc1}] = [P_\theta]^{-1}[F_{0dq1}] \qquad \text{(C-3)}$$

In the synchronously rotating reference frame where the frame rotates at speed ω, the angle $\theta = \omega t$.

APPENDIX D

Derivatives of the stator currents

From Park's orthogonal transform (Appendix C),

$$i_{d1} = \sqrt{2/3}[i_{AL}\cos\theta + i_{BL}\cos(\theta - \lambda) + i_{CL}\cos(\theta + \lambda)] \qquad \text{(D-1)}$$

Hence

$$pi_{d1} = \sqrt{2/3}[pi_{AL}\cos\theta + pi_{BL}\cos(\theta - \lambda) + pi_{CL}\cos(\theta + \lambda) - i_{AL}\omega\sin\theta - i_{BL}\omega\sin(\theta - \lambda) - i_{CL}\omega\sin(\theta + \lambda)] \qquad \text{(D-2)}$$

$$i_{q1} = \sqrt{2/3}[i_{AL}\sin\theta + i_{BL}\sin(\theta - \lambda) + i_{CL}\sin(\theta + \lambda)] \qquad \text{(D-3)}$$

Hence

$$pi_{q1} = \sqrt{2/3}[pi_{AL}\sin\theta + pi_{BL}\sin(\theta - \lambda) + pi_{CL}\sin(\theta + \lambda) + i_{AL}\omega\cos\theta + i_{BL}\omega\cos(\theta - \lambda) + i_{CL}\omega\cos(\theta + \lambda)] \qquad \text{(D-4)}$$